NJC

ROYAL SOCIETY OF CHEMISTRY

PAPER

View Article Online
View Journal | View Issue

Cite this: *New J. Chem.*, 2021, **45**, 1853

FRET based ratiometric switch for selective sensing of Al^{3+} with bio-imaging in human peripheral blood mononuclear cells†

Sangita Das, *[a] Partha Pratim Das, [b] James W. Walton, [a] Kakali Ghoshal,[c] Lakshman Patra[d] and Maitree Bhattacharyya[c]

In this work, a triphenylamine and rhodamine-B (donor–acceptor) hybrid switch (TPRH) was rationally designed, synthesised and characterised as a novel fluorescence resonance energy transfer (FRET) ratiometric fluorescent chemosensor for specific sensing of Al^{3+} over other important metal ions in mixed aqueous solution. We proposed that the sensor in hand (TPRH) is non-toxic and can be successfully employed to detect the Al^{3+} ion in human peripheral blood mononuclear cells (PBMCs), showing intracellular 'FRET-ON' mechanism. The orientation of the probe was designed in such a way that the fluorescence (or Förster) resonance energy transfer (FRET) proceeded from the 'donor moiety' triphenylamine to the 'accepter moiety' rhodamine-B. This fluorescent probe was found to be highly selective towards Al^{3+} over other important guest metal ions, including Fe^{3+} and Cr^{3+}. Considering the adverse effects of Al^{3+} ions on human health and also on the environment, the development of sensitive and specific tools for the detection of Al^{3+} ions is of great value. The limit of detection (LOD) of TPRH was found to be in the order of 10^{-8} M. The TPRH–Al^{3+} complex showed reversible binding with demetallation in the presence of EDTA. In accordance with this reversibility, the fluorescence output at 576 nm from two active chemical inputs, namely, Al^{3+} and EDTA, followed a truth table of an INHIBIT logic gate. Moreover, cytotoxic studies found that the probe was safe to use in a biological system with good cell membrane permeability. More importantly, the bio-imaging of living human peripheral blood mononuclear cells (PBMCs) showed that TPRH could be used as an effective fluorescent probe for a prominent ratiometric *in vitro* detection of the transition trivalent metal ion Al^{3+}. We evidenced a significant ($p < 0.05$) shift from blue to red fluorescence when Al^{3+} was added to the cell suspension, thus proving TPRH as a good candidate to detect intracellular Al^{3+}.

Received 12th November 2020,
Accepted 14th December 2020

DOI: 10.1039/d0nj05546h

rsc.li/njc

Introduction

Recently, the selective and sensitive detection of metal ions with smart fluorescence tools has attracted significant attention.[1–7] Metal ions play varied and important roles in living organisms as well as in the environment. These roles are often directly related to human health and global pollution problems. Hence, there is a great need to develop innovative chemosensing tools to monitor the concentrations of these ions. Aluminium is the third most abundant element in the Earth's crust. It is a nonessential metal for bio-organisms and has significant toxicity. Aluminium salts are neurotoxic and have been associated with Parkinson's disease[8] and Alzheimer's disease.[9] Furthermore, Al^{3+} has been shown to lead to breaks in the DNA double-strand and to inhibit the repair of radiation-induced lesions in human peripheral blood lymphocytes.[10] It was also found that chronic exposure to Al^{3+} can be extremely damaging to patients with renal dysfunction.[11] Aluminium is widely used in our daily lives, for example, in electrical devices, building materials, food packaging, drinking water supplies and cookware. The widespread use of aluminium increases the likelihood of its release into the environment[12] and exposure to humans and animals through food and water contamination. The concentration of aluminium in natural waters can vary significantly depending on various physicochemical and mineralogical factors. According to the World Health Organization, the threshold limit of Al^{3+} in drinking water is 7.41 μM and the daily intake of aluminium should be less than 3–10 mg.[13] It is clear

[a] *Department of Chemistry, Durham University, Durham, DH1 3LE, UK. E-mail: sangita.das@durham.ac.uk*
[b] *Department of Earth System Sciences, Yonsei University, Seoul 120749, Korea*
[c] *Department of Biochemistry, University of Calcutta, 35 Ballygunge Circular Road, Kolkata 700019, India*
[d] *Department of Chemistry, Jadavpur University, Jadavpur, Kolkata, India*

† Electronic supplementary information (ESI) available: See DOI: 10.1039/d0nj05546h

that, due to the hazardous potential of aluminium, the development of tools to detect trace levels of Al^{3+} is of paramount importance.

The gold standard in fluorescence sensing is the ratiometric analysis of two wavelengths, which allows not only the sensing of analytes without the need to know the concentration of the probe, but also the precise measurement of the intensities of two emission peaks, which overcomes the issue of quenching of emission by exogenous species with a good ratiometric value. There are several examples of non-ratiometric fluorescence and colorimetric Al^{3+} sensors, which undergo spectroscopic changes upon metal binding.[14] Improved sensors, which give a ratiometric response to Al^{3+}, have been reported, but most of them suffer from either pH dependence[15] or a lack of selectivity over other ions[16] and FRET based ratiometric bio-imaging is rare.[17] FRET is a non-radiative process, in which excited state energy transfer occurs from the donor fluorophore to the acceptor fluorophore through dipole–dipole and/or multipolar interactions.

FRET containing a potent molecular switch is extremely sensible in cell physiology and exhibits a fast reaction time, optical therapy and more importantly ultra-sensitive sensing in molecules and/or ionic species.[18] Fluorescent switches that can instantaneously recognise biologically and environmentally important ions by fluorescence imaging have become essential in various fields such as medicine and chemical science.[19] In this regard, fluorescence chemosensors provide significant advantages such as high sensitivity and specificity and a prompt response for real-time monitoring of the activities of the guest analytes inside living cells.[20] However, it is a prime requirement to study the bio-imaging mechanism by using small FRET molecular fluorophores, which indicates that aluminium ions cause aluminium-induced human diseases. In this aspect, rhodamine-based compounds are attracting considerable interest for cell imaging applications due to their unique change in fluorescence emission with spirolactam ring opening after the addition of guest cation.[21] Reports on FRET based triphenylamine–rhodamine blended probes which can specifically detect intracellular Al^{3+} are extremely rare. Therefore, in view of the recent chronic exposure to Al^{3+} and its significant toxicity, it is urgent to develop promising fluorescent tools that can selectively detect trace levels of Al^{3+}. In continuation of our previous work on fluorescence sensors,[22] herein, we have designed, synthesised and characterised a new rhodamine–triphenylamine-based FRET sensor, TPRH, for the selective detection of Al^{3+}.

We have designed the probe keeping in mind that it will exhibit FRET after selective binding with Al^{3+} in mixed aqueous medium. To enhance this mechanism, we have chosen triphenylamine as the donor (D) and rhodamine as the accepter (A), and also added a linker, ethylenediamine (ED), to make an arrangement D–ED–A. This architecture of the probe is responsible for making the binding site closer after interaction with Al^{3+} and to initiate the FRET process ON.

TPRH exhibits a response in its UV absorption and fluorescence emission spectra upon the addition of Al^{3+} with a limit of detection (LOD) of 10^{-8} M and high selectivity towards Al^{3+}. The bio-imaging experiments evidenced that TPRH could successfully measure Al^{3+} that has been loaded in the cell suspension, without damaging the cells.

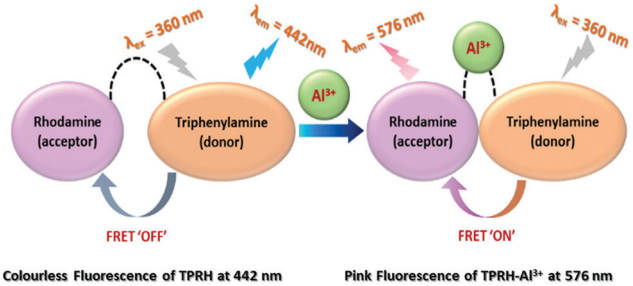

Scheme 1 TPRH sensing of Al^{3+} *via* a FRET mechanism.

The response to Al^{3+} likely arises from the modulation of FRET between triphenylamine (donor) and rhodamine (acceptor) within the sensor framework (Scheme 1). The two emission peaks used for the ratiometric analysis have a large difference in wavelength (ΔI = 134 nm), which avoids any issues of interference. Moreover, an INHIBIT logic gate was developed with two chemical inputs (Al^{3+} and EDTA) and fluorescence output at 576 nm.

Results and discussion

Synthetic procedures

The synthetic route to TPRH is shown in Scheme 2. Triphenylamine was converted to 4-(diphenylamino)benzaldehyde according to a literature procedure,[23] before being reacted with ethylenediamine, thus affording 4-(((2-aminoethyl)imino)methyl)-*N*,*N*-diphenylaniline (**1**). The rhodamine derivative **2** was synthesised according to a literature procedure.[24] The reaction of

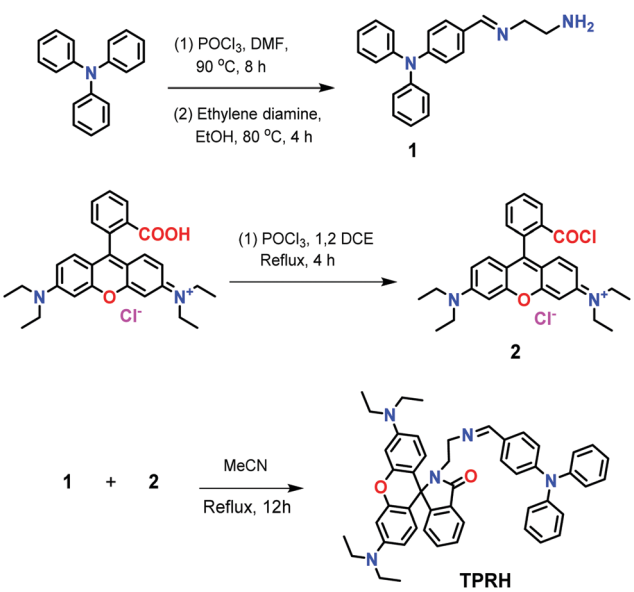

Scheme 2 Synthesis of the receptor TPRH.

intermediates **1** and **2** in refluxing acetonitrile gave the final probe, TPRH. Novel compounds **1** and **TPRH** were characterised *via* multinuclear NMR spectroscopy and HRMS (Fig. S9–S14, ESI†).

Photophysical studies

The effect of the addition of various ions to a solution of TPRH was initially investigated by the naked eye, during which it was noted that the addition of Al^{3+} salts to the colourless TPRH solution led to the appearance of an intense prominent red colour. This result encouraged us to focus on the sensing behaviour of TPRH towards Al^{3+}.

A series of photophysical studies were carried out, which included UV/vis absorption and fluorescence emission titration, along with selectivity and binding LOD studies. pH dependence and reversibility were also investigated. Furthermore, the new sensor was explored in a molecular logic gate application and as a potential solid state dip stick device to detect Al^{3+}. Unless otherwise stated photophysical studies were carried out in a mixed methanol/aqueous solution ($MeOH/H_2O$, 1/4, v/v) of TPRH (20 μM) containing 10 mM HEPES buffer at pH 7.2 and 25 °C. Solutions of ionic salts (metal perchlorates or metal chlorides) were prepared in the same aqueous buffer at pH 7.2.

UV-vis studies

In the absence of any guest analytes, the solution of TPRH exhibits characteristic absorption bands at 275 nm and 352 nm. The absence of absorption at 550 nm indicates that the probe is stable in solution phase in the closed spirolactam form. Upon the incremental addition of a solution of $AlCl_3$ (0–30 μM final concentrations), the peaks at 275 nm and 352 nm gradually decrease and a new peak appears at 550 nm, which is characteristic of the opening of the spirolactam ring (Fig. 1a). The associated change in colour of the TPRH solution from colourless to a deep pink-red colour was clearly visible to the naked eye (Fig. 1a, inset). To investigate the selectivity of TPRH towards Al^{3+}, some other selected guest metal ions (up to 5 equivalents) were titrated into a solution of TPRH. None of these guest analytes, including Na^+, K^+, Ca^{2+}, Mg^{2+}, Fe^{3+}, Co^{2+}, Ni^{2+}, Cu^{2+}, Zn^{2+}, Pb^{2+}, Cd^{2+}, Hg^{2+}, Ni^{2+}, Cr^{3+} and Mn^{2+}, exhibited notable changes in the UV-vis profile (Fig. 1b). These results show that TPRH possesses excellent selectivity towards Al^{3+} and augurs well for its use as a highly specific colorimetric sensor.

This result is in contrast to those of many other Al^{3+} sensors, which typically show interference from other metal cations, particularly Mn^{2+}, Ca^{2+}, Cr^{3+} and Fe^{3+}. The addition of Al^{3+} to TPRH exhibits a linear response in the absorption intensity at 550 nm, with an R^2 value of 0.998 (Fig. S1, ESI†) and a limit of detection (LOD) of 3.5×10^{-8} M. An association constant (K_a) of 5.9×10^5 M^{-1} was obtained using the Benesi–Hildebrand equation (Fig S2, ESI†).

Fluorescence studies

The response of TPRH to Al^{3+} was also investigated *via* fluorescence emission titration. In a similar way to the UV/vis studies, Al^{3+} was titrated into a solution of TPRH and the fluorescence emission was measured, following excitation at 350 nm. In the absence of the guest analyte, the free receptor displays a prominent emission signal at 442 nm from the triphenyl moiety and no peak at 576 nm, which indicates a stable spirolactam rhodamine B (Fig. 2a). A photoluminescence quantum yield of Φ = 0.21 was calculated (see the ESI†). Upon the incremental addition of Al^{3+} into the solution a reduction in emission intensity at 442 nm was observed with the appearance of a new red-shifted peak at 576 nm (Fig. 2a). The resultant emission spectra reveal an isoemissive point at 547 nm and allows ratiometric analysis to be conducted by comparing the peaks at 576 and 442 nm. The ratio of these two emission intensities (I_{576}/I_{442}) holds a good linear relationship, with an R^2 value of 0.999 (Fig. S3, ESI†). This linearity was maintained up to 1.2 equiv. of [Al^{3+}], after which further addition of Al^{3+} led to no further increase in the emission intensity ratio (Fig. S3a, ESI†). The large change in I_{576}/I_{442} (0.1 to 2.5) allows a facile analysis of the ratiometric signal, a further improvement of previously reported ratiometric Al^{3+} sensors. The LOD of TPRH toward Al^{3+} was estimated from the fluorescence titration[25] to be 6.7×10^{-8} M (Fig. S4, ESI†).

In order to gain a deeper insight into the stoichiometry of Al^{3+} binding with TPRH, a Job's plot experiment was performed by combining solutions of $AlCl_3$ and TPRH at various molar ratios and measuring the fluorescence emission ratio (Fig. S5, ESI†).

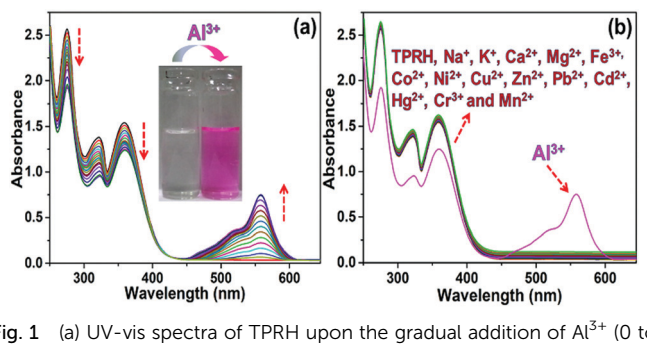

Fig. 1 (a) UV-vis spectra of TPRH upon the gradual addition of Al^{3+} (0 to 1.5 equivalents), (b) UV-vis spectra of TPRH upon the addition of 5 equivalents of the stated guest cations. TPRH (20 μM) in $MeOH/H_2O$ (1/4, v/v), HEPES buffer (10 mM), pH 7.2, 25 °C.

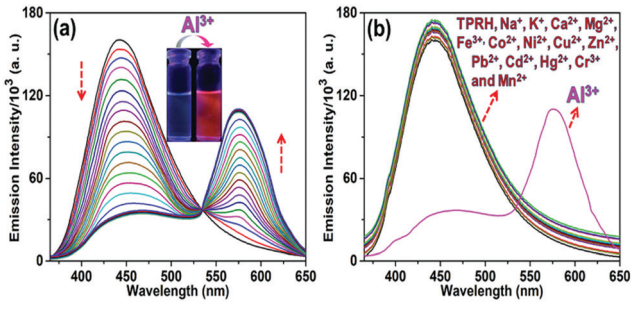

Fig. 2 (a) Changes of the emission spectra of TPRH upon the gradual addition of Al^{3+} (0 to 1.5 equivalents), (b) Changes of the emission spectra of TPRH upon the addition of 5 equivalents of the stated guest analytes. TPRH (20 μM) in $MeOH/H_2O$ (1/4, v/v), HEPES buffer (10 mM), pH 7.2, 25 °C, λ_{ex} = 350 nm.

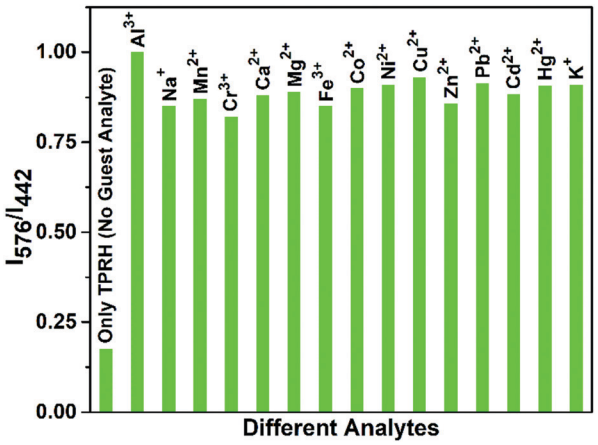

Fig. 3 A comparative study of normalized intensity ratio after the addition of different analytes (5 equivalents) in the solution of TPRH (20 μM) in the presence of Al^{3+} (2 equivalents). MeOH/H_2O (1/4, v/v) solution, HEPES buffer (10 mM), pH 7.2, 25 °C, λ_{ex} = 350 nm.

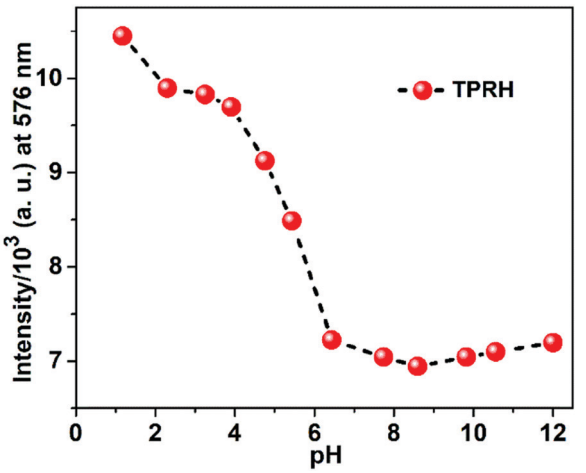

Fig. 4 Fluorescence response of TPRH at 576 nm (20 μM, λ_{ex} = 350 nm) as a function of pH in CH_3OH–H_2O (1 : 4, v/v, 25 °C); the pH was adjusted by using 1 M HCl or 1 M NaOH aqueous solution.

From the Job's plot, a 1 : 1 binding stoichiometry was determined between TPRH and Al^{3+}. Mass spectrometry ($HRMS^+$) adds further support to 1 : 1 binding, with the observation of a peak at *m*/*z* 926.26, corresponding to the molecular weight of $[TPRH + Al^{3+} + 3H_2O + 3^{35}Cl^- + H^+]^+$ (Fig. S15, ESI†). A ^1H NMR titration experiment of TPRH in the presence of Al^{3+} was also performed, which establishes the interaction between TPRH and Al^{3+}(Fig. S16, ESI†). The selectivity of TPRH was investigated by fluorescence emission. The addition of a range of metal cations (Na^+, K^+, Ca^{2+}, Mg^{2+}, Fe^{3+}, Co^{2+}, Ni^{2+}, Cu^{2+}, Zn^{2+}, Pb^{2+}, Cd^{2+}, Hg^{2+}, Ni^{2+}, Cr^{3+} and Mn^{2+}) to a solution of TPRH caused very little change in fluorescence emission and no species gave rise to a characteristic emission band at 576 nm, indicative of the spirolactam ring opening (Fig. 2b).

Furthermore, in a competition assay, a solution of TPRH and Al^{3+} was prepared and the potential competitor metal ions were added (5 equivalents). The emission at 576 nm was monitored and showed that no competitor ion was able to significantly perturb the observed fluorescence, indicating that the TPRH:Al^{3+} complex is stable towards competing ions (Fig. 3). Taken together, these results demonstrate that TPRH has great potential as a selective Al^{3+} sensor with high levels of sensitivity.

pH studies

In order to investigate the applicability of the probe in biological and environmental applications, the pH dependence of TPRH was examined using fluorescence titration. A solution of TPRH was monitored by fluorescence as the pH was adjusted from 1 to 12 using HCl and NaOH solutions (Fig. 4).

It was found that the probe is sensitive to acidic environment, with an increase in fluorescence observed below pH 6, which is likely due to acid catalysed ring opening. In neutral and alkali solutions, the probe is stable and not sensitive to pH changes, highlighting its potential for biological and environmental applications, where pH > 6 is typically encountered. These results indicate that the probe can be used in basic, near-neutral and slightly acidic conditions, but at a lower pH the spirolactam ring opens even in the absence of Al^{3+} due to protonation. The probe is stable at a pH greater than 6.2, which is found in the majority of cellular applications. At a lower pH, there is pH interference, which we acknowledge in this manuscript. Our continued work in this area aims at developing probes that can operate throughout the pH scale, but this has not been achieved yet. Despite this, the operation in the pH range of 6.2–12 allows successful measurement in most applications.

Reversibility studies

An essential feature of any chemosensor is its ability to be reversible in its sensing. To test reversibility, a solution of the TPRH:Al^{3+} complex was prepared and Na_2EDTA solution was added incrementally (Fig. 5). Upon the addition of Na_2EDTA, the pink-red colour of TPRH–Al^{3+} gradually disappeared until a

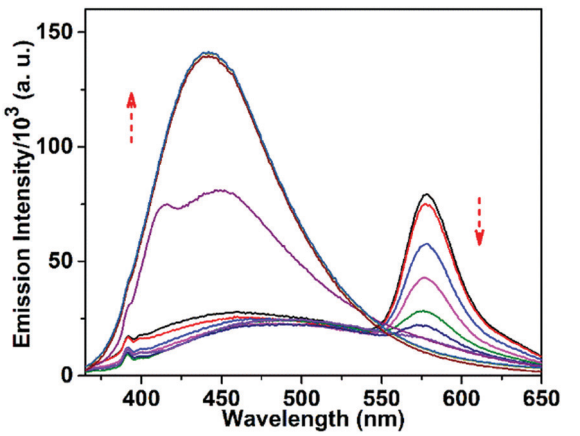

Fig. 5 Fluorescence titration spectra of TPRH–Al^{3+} (10 μM) upon increasing the concentration of Na_2EDTA (0 to 6 equivalents). In MeOH/H_2O (1/4, v/v) solution, HEPES buffer (10 mM), pH 7.2, 25 °C, λ_{ex} = 350 nm.

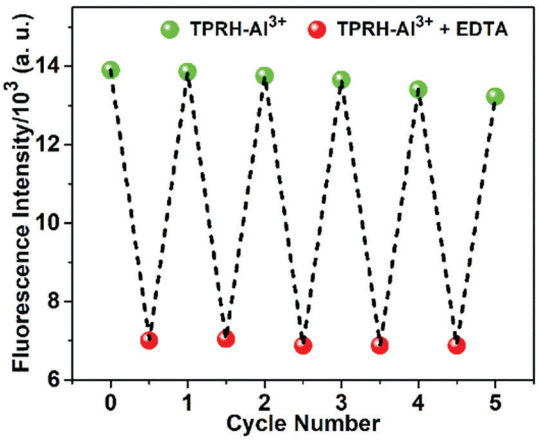

Fig. 6 The fluorescent "ON–OFF" cycles of TPRH at 576 nm upon alternating addition of Al^{3+} and EDTA in mixed aqueous medium. TPRH (10 μM) in MeOH/H_2O (1/4, v/v), HEPES buffer (10 mM), pH 7.2, 25 °C.

colourless solution was observed. From the fluorescence spectrum it is observed that, upon the addition of EDTA, the emission intensity at 576 nm gradually decreased and the restoration of the original peak of TPRH was observed at 442 nm (Fig. 5).

This indicates that the stability of the TPRH–Al^{3+} complex is lower than that of the Al–EDTA complex and that the sensing ability of TPRH is reversible. Reversibility was further explored by using this solution containing the EDTA:Al^{3+} complex and unbound TPRH and adding Al^{3+} for the second time. Upon the addition of Al^{3+}, fluorescence at 576 nm was restored, with disappearance of the peak at 442 nm. Successive cycling of Na_2EDTA and $AlCl_3$ was carried out and full reversibility was observed for six cycles, with only around 5% loss of the maximum emission and full retention of the ratiometric response to Al^{3+} (Fig. 6).

Potential binding mechanism

The chemosensor TPRH contains two potential fluorophores: triphenylamine and rhodamine-B fragments. These two chromophores, separated by the ethylenediamine linker, have the potential to display fluorescence resonance energy transfer (FRET) when they are close in space. In the free, unbound state of TPRH, the rhodamine unit is in the spirolactam form. At an excitation wavelength of 350 nm, light is absorbed and emitted solely by the triphenylamine unit, with no FRET observed. Upon Al^{3+} binding, most likely to the hard-acid donors of the imine N and amide O, the spirolactam ring opens and emission is observed at 576 nm due to the FRET between the donor triphenylamine and the acceptor rhodamine units.

Since Al^{3+} facilitates FRET, it is hypothesised that Al acts to coordinate both rhodamine and triphenylamine units (through a bridging H_2O), bringing the fluorophores close in space and allowing FRET. The FRET efficiency was calculated to be 44% for the aluminium-bound complex (see the ESI,† Fig. S6). As a result of the FRET process, emission is observed from the rhodamine unit at 576 nm and the ratiometric analysis of the emissions at 576 nm and 442 nm allows for Al^{3+} quantification. The origin of selectivity towards Al^{3+} over other metal cations is

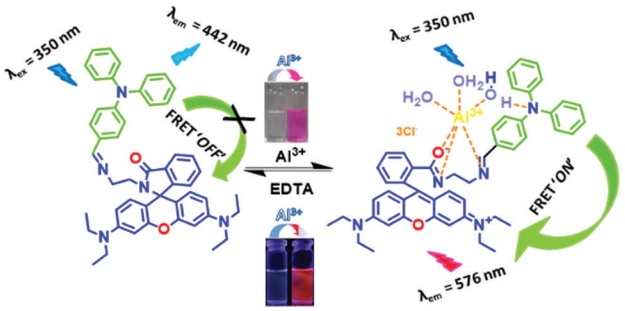

Scheme 3 Proposed FRET-based sensing strategy of TPRH with Al^{3+}.

not clear at this stage, but it may be due to the size of the binding cavity provided by the rhodamine and triphenylamine units. Scheme 3 shows the postulated binding mechanism of the probe TPRH with Al^{3+}.

Cytotoxic effects of the probe and its Al^{3+} complex

Cell viability is presented in Fig. 7, where the TPRH concentration of up to 50 μM shows around 56.67% (without Al^{3+}) and 53.22% (with 10 μM Al^{3+}) of viable cells, indicating that the probe is safe to use in a biological system. We used 10 μM TPRH solution for the imaging which showed a high number of viable cells (86.88% without Al^{3+} and 81.23% with Al^{3+}), indicating its nontoxic nature. Cell viability was calculated using the following equation:

$$\%\ \text{of Cell Viability} = \frac{(\text{Absorbance of treatment group-blank})}{(\text{Absorbance of control group-blank})} \times 100$$

TPRH has good cell permeability as well as stability at biological pH (7.4). Our MTT data indicate its safe and nontoxic nature towards cells. It does not cause cell damage such as swelling or lysis. TPRH is highly sensitive towards Al^{3+} and doses as low as 10 μM can be easily detected *via* fluorescence

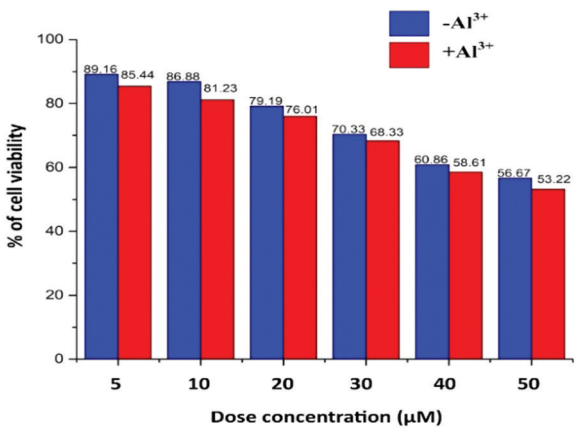

Fig. 7 Percentage of viable human peripheral blood mononuclear cells (PBMCs) over the TPRH concentration range of 5–50 μM in the presence and absence of Al^{3+}. Cells were incubated for 30 minutes at 37 °C in the dark.

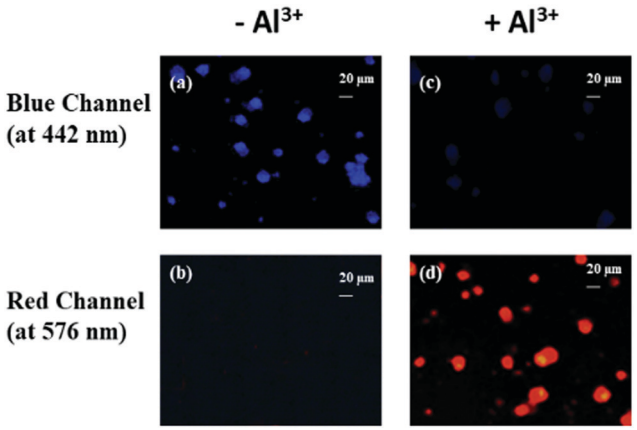

Fig. 8 Fluorescence images (40×) of human PBMCs treated with (c and d) and without (a and b) Al^{3+} (10 μM) along with 10 μM TPRH. Images were taken in the blue (emission at 442 nm) and red (emission at 576 nm) channels. λ_{ex} = 350 nm. TPRH (10 μM) could successfully detect Al^{3+} in cells and the fluorescence has shifted from blue to red, whereas no significant red signals were detected when Al^{3+} is not present.

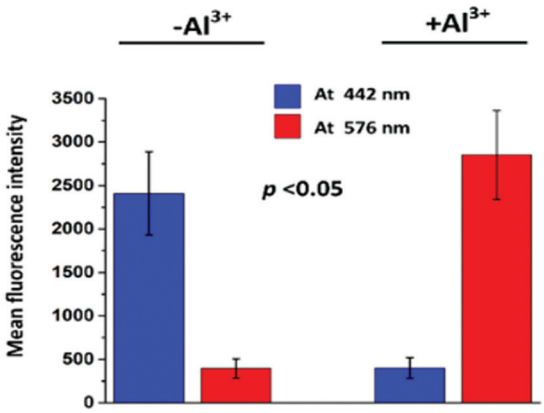

Fig. 9 The mean fluorescence intensities were measured using ImageJ, which shows a significant ($p < 0.05$) shift from blue (intensity = 401 ± 118) to red (intensity = 2851 ± 512) fluorescence, when Al^{3+} was added. When there was no Al^{3+} present blue fluorescence (intensity = 2408 ± 477) was significantly ($p < 0.05$) more visible than red fluorescence (intensity = 396 ± 110). The fluorescence intensity of individual cells was measured (15 cells per condition) and statistical analyses were done using OriginPro 9 software.

microscopy. Therefore, this fluorescence probe is safe to use and non-toxic in the detection of Al^{3+} in biological samples.

Bioimaging

An ideal approach for designing experiments would be conducting bioimaging on both primary cells and secondary cell lines. Since primary cells are more sensitive and represent a biological system more accurately than secondary cell lines, we designed this study on primary human PBMCs.

Although replicating this experiment on cell lines may provide more insights for comparison, we did not perform those experiments, which is a limitation in this study. Fig. 8 depicts the fluorescence images of human PBMCs treated with and without Al^{3+} (10 μM) in combination with 10 μM TPRH. Here, the cells exhibit significant blue fluorescence and very little or no red fluorescence (Fig. 8a and b, respectively), when treated with only TPRH and not Al^{3+}, but, remarkably, after the addition of Al^{3+} a distinct red intensity was observed, with a considerably redundant blue intensity (Fig. 8c and d, respectively), indicating the interactions between TPRH and Al^{3+}.

The size chart for the cells is also presented (20 μm) in Fig. 9. In the blue channel (at 442 nm), TPRH exhibited sharp intensities (2408 ± 477) when the cells were not treated with Al^{3+}. In the red channel (at 576 nm) almost negligible fluorescence intensities were found (396 ± 110) for Al^{3+} untreated samples. However, when Al^{3+} was added a significant increase ($p < 0.05$) in red fluorescence (2851 ± 512) was observed. The blue fluorescence was significantly ($p < 0.05$) diminished (401 ± 118) after the addition of Al^{3+}. These results strongly suggest that TPRH is a precise and convenient fluorescent probe to measure Al^{3+} in the biological system.

Solid state dipstick devices

Prompted by the successful use of TPRH as a selective Al^{3+} sensor, we decided to fabricate a simple device for detecting Al^{3+}. For this application, we used a simple dipstick method, in which a test strip (a silica TLC plate) was immersed in a solution of TPRH (0.1 mM, MeOH : H_2O 1 : 4) and then left to dry in air. When the strip was again immersed in a solution of Al^{3+} (0.01 mM), a prominent change of colour could easily be seen by the naked eye (colourless to pink-red, Fig. 10a), and under a handheld 365 nm UV lamp, a clear change in the emitted light was observed (Fig. 10b). The distinct colour change provides a quick and easy method for qualitative detection of Al^{3+}, without the need for any expensive spectrometers. With further development, a similar device could be used for real-time aluminium detection in field studies.

Molecular logic gates

Logic gates can be used as fundamental microdevices for electronic components. They accept small molecules as inputs and produce fluorescence outputs.[26] There are 16 different types of logic gates that can be produced with two inputs and one output.[27] In this work, we developed an INHIBIT logic gate based on two inputs Al^{3+} and EDTA with the fluorescence

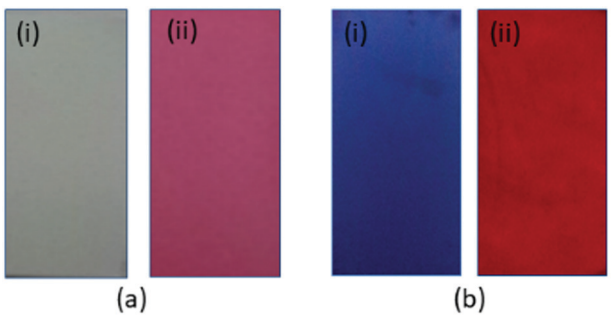

Fig. 10 Colour changes of TPRH on the test paper in the (i) absence and (ii) presence of Al^{3+} under (a) ambient light and (b) a handheld 365 nm UV lamp, respectively.

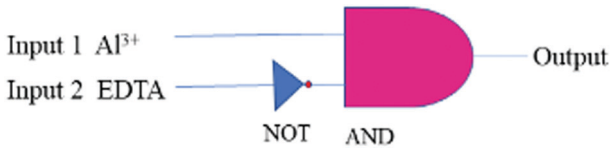

Fig. 11 General representation of the 'INHIBIT' logic gate.

emission at 576 nm as the output. This combination follows an INHIBIT truth table (Table S1, ESI†). This logic gate system is generally represented with Boolean algebra using binary codes 0 and 1, where '0' represents the fluorescence property for the inactive state 'NO'/'OFF' and '1' stands for the active state 'YES'/'ON' of the TPRH probe. The results of this study show that, in the absence of any chemical input (no guest analyte), TPRH shows no noticeable emission at 576 nm, *i.e.* output 0 (OFF/NO-state). The addition of INPUT 1 (Al^{3+}) displays prominent fluorescence at 576 nm, *i.e.*, output 1 (ON/YES-state). The application of both INPUT 1 and INPUT 2 (EDTA) together showed no visible fluorescence at 576 nm, *i.e.*, output 0 (OFF/NO-state).

This system represents an INHIBIT logic gate for TPRH, which is depicted in Fig. 11. These results show a system that mimics the functions of a semiconductor logic gate, where fluorescence emission spectroscopy is one of the most important techniques to monitor the output at the molecular level. The alteration of chemical inputs proves the applicability of TPRH as a FRET – lock – unlock sensing device for Al^{3+}.

Experimental

General

Chemicals and solvents were purchased from Sigma-Aldrich and used without further purification. Silica gel (100–200 mesh, Merck) was used for column chromatography. NMR spectra were recorded using a Varian VXR-400 spectrometer (^{1}H at 399.97 Hz, ^{13}C at 100.57 MHz) at 295 K in commercially available d^6 DMSO, with TMS as an internal standard. Chemical shifts are expressed in δ units and coupling constants in Hz. UV-vis spectra were recorded using a Cary 5000 high performance UV-vis-NIR spectrophotometer, controlled using the Cary WinUV software. Fluorescence was recorded with a Horiba Fluorolog-3 spectrometer using the FluorEssence software.

General method of UV-vis absorption and fluorescence emission titrations

For both UV-vis and fluorescence titrations, a stock solution of TPRH was prepared (20 μM) in CH_3OH–H_2O (1 : 4, v/v) in the presence of HEPES buffer (10 mM) solution at pH 7.2. Solutions of the guest cations were prepared using their perchlorate/chloride salts at 20 μM and buffered deionised water at pH 7.2. The absorption spectra of these solutions were recorded by means of UV-vis methods using a 10 mm pathlength quartz cuvette. Fluorescence emission was measured using a 10 mm pathlength quartz cuvette with an excitation wavelength of 350 nm.

Synthesis of compound 1 (4-(((2-aminoethyl)imino)methyl)-*N*,*N*-diphenylaniline)

Ethylenediamine (150 mg, 2.5 mmol) was added to the stirred solution of 4-(diphenylamino)benzaldehyde (546 mg, 2 mmol) in dry ethanol solvent (10 ml) and the mixture was refluxed for 4 hours. The mixture was cooled to room temperature and poured into cold water. The formed precipitate was collected through filtration and dried under vacuum. This crude material was purified by column chromatography on silica using 5% ethyl acetate in petroleum ether as the eluent. Yield: 480 mg (72%). ^{1}H NMR (400 MHz, $CDCl_3$): δ 2.88 (t, J = 5.2 Hz, 2H, CH_2), 3.64 (t, J = 5.2 Hz, 2H, CH_2), 4.95 (s, 2H, NH_2), 7.14 – 7.31 (m, 4H, *Ar*), 7.51–7.56 (m, 5H, *Ar*), 7.58–7.63 (m, 5H, *Ar*), 8.22 (s, 1H, CH═N). ^{13}C NMR (75 MHz, $CDCl_3$): δ 55.6, 59.9, 122.1, 124.0, 126.4, 126.8, 128.2, 130.4, 148.8, 150.6, 161.5. MS (ESI, positive mode): calcd for $C_{21}H_{21}N_3$ $[M + H]^+$ (*m*/*z*): 316.18; found: 316.13.

Synthesis of TPRH (3′,6′-bis(diethylamino)-2-(2-((4-(diphenylamino)-benzylidene)amino)ethyl)spiro[isoindoline 1,9′-xanthen]-3-one)

A mixture of 4-(((2-aminoethyl)imino)methyl)-*N*,*N*-diphenylaniline (**1**) (315 mg, 1.00 mmol) and *N*-(9-(2-(chlorocarbonyl)phenyl)-6-(ethylamino)-3*H*-xanthen-3-ylidene)-*N*-ethylethanaminium chloride (**2**) (468 mg, 1.00 mmol) in anhydrous acetonitrile (20 ml) was heated to reflux for 12 h. The solvent was removed under reduced pressure to give a yellow residue, which was purified by column chromatography (silica gel, 5% ethyl acetate in petroleum ether) to give TPRH as a crystalline solid (530 mg, 70%). ^{1}H NMR (400 MHz, d^6-DMSO): δ 1.08 (t, J = 6.5 Hz, 12H, CH_3), 2.46–2.42 (m, 8H, CH_2CH_2), 3.20–3.40 (m, 8H, CH_2CH_3), 6.30–6.40 (m, 6H, *Ar (rhodamine)*), 6.87 (d, 2H, J = 6.5 Hz, N = CH-*Ar*-NPh_2), 7.00–7.30 (m, 1H, *Ar (rhodamine)*), 7.05 (d, 4H, J = 6.0 Hz, N*Ph*$_2$ (*ortho-H*)), 7.11 (t, 2H, J = 6.0 Hz, N*Ph*$_2$ (*para-H*)), 7.33 (t, 4H, J = 6.0 Hz, N*Ph*$_2$ (*meta-H*)), 7.46 (d, 2H, J = 6.5 Hz, N═CH-*Ar*-NPh_2), 7.48–7.54 (m, 2H, *Ar (rhodamine)*), 7.76–7.82 (m, 1H, *Ar (rhodamine)*), 7.86 (s, 1H, CH═N). ^{13}C NMR (100 MHz, $CDCl_3$): δ 12.6, 30.9, 44.3, 58.9, 64.9, 97.8, 105.5, 108.0, 121.8, 122.6, 123.6, 123.7, 125.1, 126.3, 127.9, 128.9, 129.0, 129.3, 129.5, 129.7, 131.0, 132.3, 147.1, 148.7, 149.9, 153.3, 153.7, 161.9, 168.2, 207.1. HRMS (ESI, positive mode): calcd for $C_{49}H_{49}N_5O_2$ $[M + H]^+$ (*m*/*z*): 740.3959; found: 740.3968.

The Al^{3+} complex of TPRH

The receptor, TPRH (50 mg, 0.07 mmol) and $AlCl_3$ (12 mg, 0.09 mmol) were dissolved in methanol (7 ml) and the mixture was heated to reflux for 10 h. The reaction mixture was cooled to room temperature and a red precipitate formed, which was collected by filtration and dried in vacuum to give the title compound. MS (ESI, positive mode): calcd. for $C_{49}H_{56}AlCl_3N_5O_5$ $[TPRH + Al^{3+} + 3^{35}Cl^- + 3H_2O + H^+]^+$ (*m*/*z*): 926.31; found: 926.26.

Details of bio-imaging

Materials and methods

Venous blood (3 ml) was obtained from a healthy, male, volunteer donor (age: 30 years) with his informed consent. Peripheral blood mononuclear cells (PBMCs) were harvested by density gradient

centrifugation utilizing Histopaque-1077 gradient (Sigma). PBMCs were washed twice with ice cold PBS and then suspended in the same. The suspended cells were treated with (10 μM $AlCl_3$) and without (control vehicle) Al^{3+}. TPRH samples were prepared in PBS containing 0.5% DMSO. Both Al^{3+} treated and untreated samples were incubated with 10 μM TPRH solution for 30 minutes at 37 °C in the dark. Intracellular fluorescence intensity was detected using a fluorescence microscope (Carl Zeiss HBO 100) under 40× magnification with fluorescence emissions at 442 nm (blue channel, Filter set 49) and 576 nm (red channel, Filter set 42). Relative fluorescence intensities were calculated using ImageJ software.

MTT assay

To determine cell viability against TPRH, PBMCs were treated with different concentrations of TPRH solution (5–50 μM) with or without Al^{3+} (10 μM) for 1 hour at 37 °C against the control cell suspension (without TPRH). The cell density remained at 0.05×10^6 cells per well in a 96-well plate. 100 μl of MTT solution (5 mg ml^{-1}) was added to each well including the control and incubated for 4 hours at 37 °C. The purple coloured formazan crystals were dissolved in 100 μl DMSO and the absorbance was measured at 570 nm. Cell viability was calculated using the following equation:

$$\%\ \text{of Cell Viability} = \frac{(\text{Absorbance of treatment group-blank})}{(\text{Absorbance of control group-blank})} \times 100.$$

Conclusions

In summary, we have developed a new triphenylamine and rhodamine-B based chemosensor, which can exclusively detect Al^{3+} *via* a ratiometric fluorescence response. The selective detection of Al^{3+} by the ratiometric analysis of two emission wavelengths is important as it allows measurement without the need to know the probe concentration and is not susceptible to interference by competitor ions. The ratiometric analysis overcomes the issue of quenching by unknown contaminants. The probe, TPRH, shows excellent selectivity to Al^{3+} over a broad range of important metal ions, shows reversible binding for at least six cycles and has a limit of detection of 10^{-8} M. For some potential applications, a solid-state device was produced that exhibits a response in the presence of solutions containing Al^{3+} and an INHIBIT logic gate was generated. Overall, this new probe has long term potential to improve health and wellbeing by sensing trace amounts of Al^{3+} in mixed aqueous samples in an accurate and effective manner. TPRH can even serve as an excellent probe to detect Al^{3+} in biological systems (such as human peripheral blood mononuclear cells, PBMCs) in a nontoxic and convenient way.

Ethical declarations

All experiments were performed in accordance with the guidelines of the Calcutta University Biosafety and Ethics Committee and approved by the same. Informed consent was obtained from the human participants of this study.

Conflicts of interest

There are no conflicts to declare.

Acknowledgements

S. Das acknowledges the Newton International Fellowships Royal Society (UK) for the fellowship (ref. NIF\R1\182209).

Notes and references

1 Y. M. You, Y. J. Han, Y. M. Lee, S. Y. Park, W. W. Nam and S. J. Lippard, *J. Am. Chem. Soc.*, 2011, **133**, 11488.
2 J. Han, X. Tang, Y. Wang, R. J. Liu, L. Wang and L. Ni, *Spectrochim. Acta, Part A*, 2018, **205**, 597–602.
3 H. H. Wang, Q. Gan, X. J. Wang, L. Xue, S. H. Liu and H. Jiang, *Org. Lett.*, 2007, **9**, 4995.
4 B. Qiao, S. G. Sun, N. Jiang, S. Zhang and X. J. Peng, *Dalton Trans.*, 2014, **43**, 4626.
5 E. Ranyuk, C. M. Douaihy, A. Bessmertnykh, F. Denat, A. Averin, I. Beletskaya and R. Guilard, *Org. Lett.*, 2009, **11**, 987.
6 M. Zhang, Y. Yang, L. Y. Liu, W. X. Chang and J. Li, *Macromolecules*, 2016, **49**, 844.
7 (*a*) M. Shyamal, P. Mazumdar, S. Maity, G. P. Sahoo, G. Salgado-Morán and A. Misra, *J. Phys. Chem. A*, 2016, **120**, 210; (*b*) K. Aich, S. Das, S. Gharami, L. Patra and T. K. Mondal, *ChemistrySelect*, 2019, **4**, 8068–8073; (*c*) L. Patra, S. Das, S. Gharami, K. Aich and T. K. Mondal, *New J. Chem.*, 2018, **42**, 19076–19082; (*d*) K. Aich, S. Goswami, S. Das and C. D. Mukhopadhyay, *RSC Adv.*, 2015, **5**, 31189–31194; (*e*) S. Goswami, K. Aich, S. Das, C. D. Mukhopadhyay, D. Sarkar and T. K. Mondal, *Dalton Trans.*, 2015, **44**, 5763–5770; (*f*) S. Goswami, K. Aich, S. Das, A. K. Das, A. Manna and S. Halder, *Analyst*, 2013, **138**, 1903–1907.
8 D. P. Perl and A. R. Brody, *Science*, 1980, **208**, 297.
9 D. P. Perl, D. C. Gajdusek, R. M. Garruto, R. T. Yanagihara and C. J. Gibbs, *Science*, 1982, **217**, 1053.
10 A. Lankoff, A. Banasik, A. Duma, D. Ochniak, H. Lisowska, T. Kuszewski, S. Gozdz and A. Wojcik, *Toxicol. Lett.*, 2006, **161**, 27.
11 J. Savory, R. L. Bertholf and M. R. Wills, Aluminium toxicity in chronic renal insufficiency, *Clin. Endocrinol. Metab.*, 1985, **14**, 681–702.
12 (*a*) P. Nayak, *Environ. Res.*, 2002, **89**, 101–115; (*b*) N. Fimreite, O. O. Hansen and H. C. Pettersen, *Bull. Environ. Contam. Toxicol.*, 1997, **58**, 1–7.
13 (*a*) T. Han, X. Feng, B. Tong, J. Shi, L. Chen, J. Zhi and Y. Dong, *Chem. Commun.*, 2012, **48**, 416–418; (*b*) Z. Krejpcio and R. W. Wojciak, *Pol. J. Environ. Stud.*, 2002, **11**, 251–254; (*c*) J. Barcelo and C. Poschenrieder, *Environ. Exp. Bot.*, 2002,

48, 75–92; (*d*) T. Han, X. Feng, B. Tong, J. Shi, L. Chen, J. Zhi and Y. Dong, *Chem. Commun.*, 2012, **48**, 416–418.

14 (*a*) S. Das, M. Dutta and D. Das, *Anal. Methods*, 2013, **5**, 6262–6285; (*b*) D. Maity and T. Govindaraju, *Eur. J. Inorg. Chem.*, 2011, 5479–5485; (*c*) J.-C. Qin, X. Cheng, R. Fang, M. Wang, Z. Yang, T. Li and Y. Li, *Spectrochim. Acta, Part A*, 2016, **152**, 352–357; (*d*) L. McDonald, J. Wang, N. Alexander, H. Li, T. Liu and Y. Pang, *J. Phys. Chem. B*, 2016, **120**, 766–772; (*e*) G. R. Zou, C. X. Liu, C. Cong, Z. T. Fang, W. Yang, X. M. Luo, S. K. Jia, F. Wu and X. Zhou, *Chem. Commun.*, 2018, **54**, 13107–13110; (*f*) B. Naskar, A. Bauza, A. Frontera, D. K. Maiti, C. D. Mukhopadhyay and S. Goswami, *Dalton Trans.*, 2018, **47**, 15907–15916; (*g*) A. Sahana, A. Banerjee, S. Lohar, B. Sarkar, S. K. Mukhopadhyay and D. Das, *Inorg. Chem.*, 2013, **52**, 3627–3633.

15 (*a*) Z. Li, W. Chen, L. Dong, Y. Song, R. Li, Q. Li, D. Qu, H. Zhang, Q. Yang and Y. Li, *New J. Chem.*, 2020, **44**, 3261–3267; (*b*) X. Sun, Y.-W. Wang and Y. Peng, *Org. Lett.*, 2012, **14**, 3420–3423.

16 (*a*) K. Boonkitpatarakul, J. Wang, N. Niamnont, B. Liu, L. Mcdonald, Y. Pang and M. Sukwattanasinitt, *ACS Sens.*, 2015, **1**, 144–150; (*b*) X. Sun, Y.-W. Wang and Y. Peng, *Org. Lett.*, 2012, **14**, 3420–3423; (*c*) H. Y. Liu, T. Q. Liu, J. Li, Y. M. Zhang, J. H. Li, J. Song, J. L. Qu and W. Y. Wong, *J. Mater. Chem. B*, 2018, **6**, 5435–5442; (*d*) B. Sen, S. Pal, S. Lohar, M. Mukherjee, S. K. Mandal, A. R. Khuda-Bukhsh and P. Chattopadhyay, *RSC Adv.*, 2014, **4**, 21471; (*e*) A. Manna, D. Sain, N. Guchhaita and S. Goswami, *New J. Chem.*, 2017, **41**, 14266; (*f*) H. Liu, T. Liu, J. Li, Y. Zhang, J. Li, J. Song, J. Qu and W.-Y. Wong, *J. Mater. Chem. B*, 2018, **6**, 5435–5442; (*g*) A. E. Sadak and E. Karakuş, *J. Fluoresc.*, 2020, **30**, 213–220.

17 (*a*) A. Roy, S. Dey and P. Roy, *Sens. Actuators, B*, 2016, **237**, 628; (*b*) H. Xie, Y. Wu, J. Huang, F. Zeng, H. Wu, X. Xia, C. Yu and S. Wu, *Talanta*, 2016, **151**, 8; (*c*) Y. Zhang, Y. Fang, N.-Z. Xu, M.-Q. Zhang, G.-Z. Wu and C. Yao, *Chin. Chem. Lett.*, 2016, **27**, 1673; (*d*) D. Jeyanthi, M. Iniya, K. Krishnaveni and D. Chellappa, *RSC Adv.*, 2013, **3**, 20984; (*e*) J.-c. Qin and Z.-y. Yang, *Anal. Methods*, 2015, **7**, 2036; (*f*) S. Sinha, B. Chowdhury and P. Ghosh, *Inorg. Chem.*, 2016, **55**, 9212; (*g*) S. Goswami, A. Manna, S. Paul, A. K. Maity, P. Saha, C. K. Quah and H. K. Fun, *RSC Adv.*, 2014, **3**, 34572; (*h*) S. Das, S. Goswami, K. Aich, K. Ghoshal, C. K. Quah, M. Bhattacharyya and H.-K. Fun, *New J. Chem.*, 2015, **39**, 8582–8587.

18 (*a*) J. Fan, M. Hu, P. Zhan and X. Peng, *Chem. Soc. Rev.*, 2013, **42**, 29; (*b*) N. Kumar, V. Bhalla and M. Kumar, *Analyst*, 2014, **139**, 543; (*c*) V. Luxami, M. Verma, R. Rani, K. Paul and S. Kumar, *Org. Biomol. Chem.*, 2012, **10**, 8076; (*d*) A. K. Mandal, M. Suresh, P. Das and A. Das, *Chem. – Eur. J.*, 2012, **18**, 3906; (*e*) M. Suresh, A. K. Mandal, M. K. Kesharwani, N. N. Adarsh, B. Ganguli, R. K. Kanaparthi, A. Samanta and A. Das, *J. Org. Chem.*, 2011, **76**, 138; (*f*) H. Yu, Y. Xiao, H. Guo and X. Qian, *Chem. – Eur. J.*, 2011, **17**, 3179; (*g*) M. Kumar, N. Kumar, V. Bhalla, H. Singh, P. R. Sharma and T. Kaur, *Org. Lett.*, 2011, **13**, 1422; (*h*) W. Guo, X. Lv, J. Liu, Y. L. Liu, Y. Zhao, M. L. Chen and P. Wang, *Org. Biomol. Chem.*, 2011, **9**, 4954; (*i*) X. Zhou, F. Su, H. Lu, P. Senechal-Willis, Y. Tian, R. H. Johnson and D. R. Meldrum, *Biomaterials*, 2012, **33**, 171; (*j*) L. Yuan, W. Lin, Z. Cao, J. Wang and B. Chen, *Chem. – Eur. J.*, 2012, **18**, 1247; (*k*) W. Y. Lin, L. L. Long, B. B. Chen, W. S. Gao and L. Yuan, *Chem. Commun.*, 2011, **47**, 893; (*l*) C. Kar, M. D. Adhikari, A. Ramesh and G. Das, *Inorg. Chem.*, 2013, **52**, 743.

19 (*a*) T. Schraderr and A. D. Hamilton, *Functional Synthetic Receptors*, Wiley-VCH, Weinheim, Germany, 2005; (*b*) J. P. Desvergne, A. Czarnik and W. Kluwer, *Chemosensors of Ion and Molecule Recognition*, Dordrecht, 1997; (*c*) A. W. Czarnik, *Fluorescent Chemosensors for Ion and Molecule Recognition*, American Chemical Society, Washington, DC, 1992; (*d*) R. Maınez-Ma∼nez and F. Sancenon, *Chem. Rev.*, 2003, **103**, 4419; (*e*) P. D. Beer and P. A. Gale, *Angew. Chem., Int. Ed.*, 2001, **40**, 486; (*f*) A. P. De Silva, H. Q. N. Gunaratne, T. Gunnlaugsson, A. J. M. Huxley, C. P. McCoy, J. T. Rademacher and T. E. Rice, *Chem. Rev.*, 1997, **97**, 1515; (*g*) Z. Li, W. Chen, L. Dong, Y. Song, R. Li, Q. Li, D. Qu, H. Zhang, Q. Yang and Y. Li, *New J. Chem.*, 2020, **44**, 3261–3267.

20 (*a*) U. E. Spichiger-Keller, *Chemical Sensors and Biosensors for Medical and Biological Applications*, Wiley-VCH, Weinheim, Germany, 1998; (*b*) V. Amendola, L. Fabbrizzi, F. Forti, M. Licchelli, C. Mangano, P. Pallavicini, A. Poggi, D. Sacchi and A. Taglieti, *Coord. Chem. Rev.*, 2006, **250**, 273; (*c*) K. Rurack and U. Resch-Genger, *Chem. Soc. Rev.*, 2002, **31**, 116; (*d*) P. T. Srinivasan, T. Viraraghavan and K. S. Subramanian, *Water SA*, 1999, **25**, 47.

21 (*a*) R. Zhang, F. Yan, Y. Huang, D. Kong, Q. Ye, J. Xu and Li Chen, *RSC Adv.*, 2016, **6**, 50732–50760; (*b*) Y. Zhang, S. Xia, M. Fang, W. Mazi, Y. Zeng, T. Johnston, A. Pap, R. L. Luck and H. Liu, *Chem. Commun.*, 2018, **54**, 7625–7628; (*c*) H. Izawa, S. Wakizono and J.-i. Kadokawa, *Chem. Commun.*, 2010, **46**, 6359–6361; (*d*) Y.-Y. Liang, J. Zhang, H. Cui, Z.-S. Shao, C. Cheng, Y.-B. Wang and H.-S. Wang, *Chem. Commun.*, 2020, **56**, 3183–3186; (*e*) P.-Y. Wang, X. Luo, L.-L. Yang, Y.-C. Zhao, R. Dong, Z. Li and S. Yang, *Chem. Commun.*, 2019, **55**, 7691–7694; (*f*) C. Zhang, H. Xie, T. Zhan, J. Zhang, B. Chen, Z. Qian, G. Zhang, W. Zhang and J. Zhou, *Chem. Commun.*, 2019, **55**, 9444–9447.

22 (*a*) S. Goswami, S. Das, K. Aich, B. Pakhira, S. Panja, S. Mukherjee and S. Sarkar, *Org. Lett.*, 2013, **15**, 5412–5415; (*b*) S. Goswami, K. Aich, S. Das, A. K. Das, D. Sarkar, S. Panja, T. K. Mondal and S. Mukhopadhyay, *Chem. Commun.*, 2013, **49**, 10739–10741; (*c*) S. Goswami, K. Aich, A. K. Das, A. Manna and S. Das, *RSC Adv.*, 2013, **3**, 2412–2416; (*d*) S. Goswami, K. Aich, S. Das, S. Basu Roy, B. Pakhira and S. Sarkar, *RSC Adv.*, 2014, **4**, 14210–14214; (*e*) S. Goswami, S. Das, K. Aich, D. Sarkar, T. K. Mondal, C. K. Quah and H.-K. Fun, *Dalton Trans.*, 2013, **42**, 15113–15119; (*f*) L. Patra, S. Das, S. Gharami, K. Aich and T. K. Mondal, *New J. Chem.*, 2018, **42**, 19076–19082; (*g*) S. Goswami, K. Aich, S. Das, A. K. Das, A. Manna and S. Halder, *Analyst*, 2013, **138**, 1903–1907; (*h*) S. Goswami, S. Das, K. Aich, D. Sarkar and T. K. Mondal, *Tetrahedron Lett.*, 2014, **55**,

2695–2699; (*i*) S. Goswami, S. Das and K. Aich, *Tetrahedron Lett.*, 2013, **54**, 4620–4623; (*j*) S. Goswami, S. Das, K. Aich, P. K. Nandi, K. Ghoshal, C. K. Quah, M. Bhattacharyya, H.-K. Fun and H. A. A. Aziz, *RSC Adv.*, 2014, **4**, 24881–24886; (*k*) S. Goswami, S. Das, K. Aich, D. Sarkar and T. K. Mondal, *Tetrahedron Lett.*, 2013, **54**, 6892–6896; (*l*) S. Das, K. Aich, S. Goswami, C. K. Quah and H. K. Fun, *New J. Chem*, 2016, **40**, 6414–6420; (*m*) S. Goswami, S. Das and K. Aich, *RSC Adv.*, 2015, **5**, 28996–29001; (*n*) S. Das, K. Aich, L. Patra, K. Ghoshal, S. Gharami and M. Bhattacharyya, *Tetrahedron Lett.*, 2018, **59**, 1130–1135.

23 T. Mallegol, S. Gmouh, M. A. A. Meziane, M. Blanchard-Desce and O. Mongin, *Synthesis*, 2005, 1771.

24 K. Aich, S. Goswami, S. Das, C. D. Mukhopadhyay, C. K. Quah and H. K. Fun, *Inorg. Chem.*, 2015, **54**, 7309–7315.

25 (*a*) M. Shortreed, R. Kopelman, M. Kuhn and B. Hoyland, *Anal. Chem.*, 1996, **68**, 1414; (*b*) W. Lin, L. Yuan, Z. Cao, Y. Feng and L. Long, *Chem. – Eur. J.*, 2009, **15**, 5096.

26 (*a*) Z.-H. Fu, L.-B. Yan, X. Zhang, F.-F. Zhu, X.-L. Han, J. Fang, Y.-W. Wang and Y. Peng, *Org. Biomol. Chem.*, 2017, **15**, 4115–4121; (*b*) V. Bojinov and N. Georgiev, *J. Univ. Chem. Technol. Metall.*, 2011, **46**, 3–26; (*c*) D. C. Magri, G. J. Brown, G. D. McClean and A. P. de Silva, *J. Am. Chem. Soc.*, 2006, **128**, 4950–4951.

27 P. Burger, *Digital design: a practical course*, Wiley, New York, 1988.

